# WDS 09144+5241: CCD Observations and Orbital Solutions

Chance Crigler, Beatrice Millar, and Hagan Hensley
Stanford Online High School, Stanford, California

**Abstract:** Using a robotic telescope, we measured WDS 09144+5241 STF 1321AB to have a position angle 98.37° and separation of 17.01" on Jan 16, 2018. Using a different robotic telescope, we measured a position angle 98.56° and separation of 17.01" on Feb 19, 2018. Combining our measurements with those of past astronomers, we conclude that the orbit of this star is beginning to deviate from the solution proposed by Kyongae Chang in 1972. By identifying a trend in the residuals of historical measurements relative to the orbital fit, we are able to improve this system's orbital parameters.

## Introduction

Binary stars are important for astronomy because the combined mass of the stars can be determined using the solved orbit of the system. In combination with other methods such as spectroscopy, the individual star masses can be found. This helps to refine the mass-luminosity relationship, which makes possible further classifications of other stars.

Short-arc binaries are systems for which less than a third of the orbit has been observed. This leads to uncertainty in the orbital period as well as the other six orbital parameters. WDS 09144+5241 is one such short-arc binary. It has been observed for 197 years of its predicted 975-year period, and has an orbit grade of 4.

According to the 6th Orbit Catalog grading method, Grade 1 orbits have the highest certainty of their orbital parameters, because measurements show a clear and complete ellipse traced out by the motion of the dimmer secondary star relative to the brighter primary (Hartkopf, 2001). In Figure 1, a sample Grade 1 orbit is shown on the left next to Kyongae Chang's orbital solution for WDS 09144+5241 on the right (Chang, 1972). The cross represents the primary star, and the dots trace out the position of the secondary relative to the primary as seen from Earth. The color of the

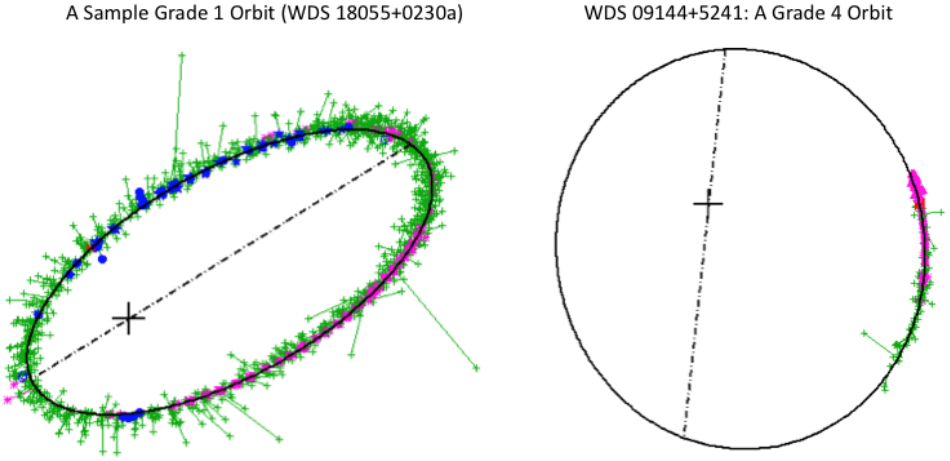


*Figure 1. A sample Grade 1 orbit (left) next to the Grade 4 Orbit of WDS 09144+5241 (right).*

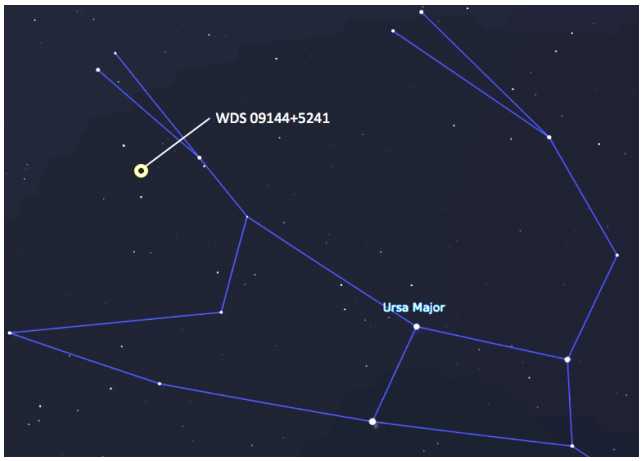


*Figure 2. Image of WDS 09144+5241 STF 1321 AB in Stellarium.*

measurements indicates their type: green data points were measured with a micrometer, pink are photographic, and blue are speckle interferometry. A line is drawn from each measurement to the projected position of the secondary star on the corresponding date according to the orbital solution. This line is called the residual. In general, the green micrometer measurements have the largest residuals, which is expected because they represent the least accurate type of measurement.

A January 2018 study of WDS 09144+5241 noted a deviation of the most recent pink photographic measurements from the black line of Kyongae Chang's 1972 orbital solution (Bush 2018). Zoomed in, these measurements appear to be further to the right of the orbital solution as time advances.

## Location of WDS 09144+5241

WDS 09144+5241 is located at 09H 14M 22.79" +52° 41' 11.8" in the northern hemisphere in Ursa Major, as shown in Figure 2. The primary star's magnitude is 7.79, the secondary star's magnitude is 7.88.

## Proper Motion

The proper motion (PM) of a star system is a measure of its change in Right Ascension (RA) over time, and its change in Declination (Dec) over time. The PM of WDS 09144+5241 listed in Table 1 was retrieved from the 2018 Gaia Survey Data Release 2 (DR2). The PM values shown in the WDS catalog for this system look very different, but actually they are not as discrepant as they appear. This is because there are only 3 characters reserved for PM in each of RA and Dec in the WDS catalog. Usually, these three characters are sufficient, because very few stars appear to be moving as quickly as this pair. At 21 lightyears (ly) distant, WDS 09144+5241 is relatively close to Earth, which augments its apparent velocity. In large-PM cases such as this one, the WDS catalog lists the PM not in milliarcseconds per year (mas/year) but in milliarcseconds per *tenth* of a year.

The values in Table 1 can be used to determine the proper motion ratio of the two stars (Harshaw 2016). The PM in RA and Dec are conceptualized as components of a two-dimensional vector. First, the PM vector of the secondary is subtracted from that of the primary star. The magnitude of the resulting difference vector is then divided by the magnitude of the longer of the two PM vectors. Figure 3 shows a visual representation of the situation. For WDS 09144+5241, the magnitude of the ratio is 0.066. This low value indicates that the stars are moving together through space, which is necessary for them to be gravitationally bound to each other. Indeed, Harshaw has shown that such Common Proper Motion (CPM) systems are often binary (Harshaw, 2014).

## Star Discoverer

WDS 09144+5241 was discovered by Friedrich Georg Wilhelm von Struve in 1821. Struve and his parents, Maria Emerentia Wiese and Jacob Struve, lived in Hamburg, Germany. Struve later moved to Russia (modern day Estonia) and became a teacher at Dorpat University, which is where he likely discovered this system (Encyclopaedia Britannica, 1998). Friedrich Georg Wilhelm von Struve catalogued almost 3000 double stars, and published his findings in *Stellarum Duplicum Et Multiplicum Mensurae Micrometricae,* or "Micrometric Measurements of Double and Multiple Stars". He also worked in the field of geodetic surveying and created the Struve Geodetic Arc, a 2880 km

*Table 1. Proper motion and parallax data of WDS 09144+5241 from the April 2018 Gaia Data Release compared to the proper motion listed in the WDS catalog.*

| | Gaia DR2 PM in RA (mas/year) | WDS PM in RA (mas / tenth of a year) | Gaia DR2 PM in Dec (mas/year) | WDS PM in Dec (mas/tenth of a year) | Gaia DR2 distance from Earth (ly) |
|---|---|---|---|---|---|
| Primary | -1546.1 | -153 | -569.1 | -56 | 20.66 ± 0.0054 |
| Secondary | -1573.1 | -155 | -660.1 | -66 | 20.66 ± 0.0048 |

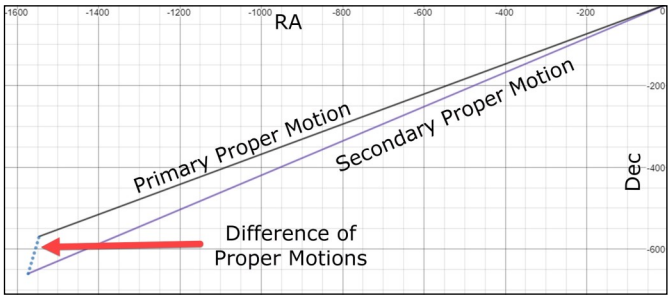


*Figure 3. Proper motion of WDS 09144+5241.*

long measurement of a meridian. This helped improve the model of the Earth and its topography (World Heritage Centre, 2018). For his efforts in these fields, he was awarded the Gold Medal of the Royal Astronomical Society (Wikipedia 2017 "Friedrich Georg Wilhelm von Struve").

## Instruments Used

The Dark Sky Observatory 17 (DSO-17), Dark Sky Observatory 14 (DSO-14) and Athabasca University Geophysical Observatory (AURT) robotic telescopes were used to image WDS 09144+5241. These telescopes were accessed via the Skynet Robotic Telescope Network, which is used by students and researchers in addition to astronomers. Skynet is mostly used to image stars, planets and to view gamma ray bursts. The DSO telescopes are set to take images of the optical afterglows of gamma-ray bursts following a command from the Swift Gamma-Ray Burst Mission. A telescope can be selected by a student or researcher to make an observation through an online request.

### *DSO-17*

The DSO-17 telescope is located in North Carolina, USA. DSO-17 has an aperture size of 43cm, F-ratio of 6.8, and a focal length of 2950 mm. It has an SBIG STL 11000M CCD camera with an FW8 filter wheel. Because of DSO-17's large aperture, it is able to capture very faint stars (Wikipedia contributors 2017 "Dark Sky Observatory").

### *DSO-14*

The DSO-14 telescope is located next to the DSO-17 telescope. DSO-14 has an aperture size of 35cm, F-ratio of 12.2, and a focal length of 4350 mm. DSO-14 is located on the same site as DSO-17 and is also used for both research and public viewings. It is fitted with an Apogee Alta U47 CCD camera, which has a back-illuminated 1024x1024 pixel array (Smith, 2009).

### *AURT*

The AURT telescope is located at Athabasca University in the province of Alberta in Canada. AURT has an aperture size of 35cm, a focal length of 3870 mm and an F-ratio of 10.9. The AURT telescope is designed to give astronomy students a first-hand experience of operating telescopes for their research (Skynet AURT, 2018). It has a Starlight Xpress SXV-M25 CCD imager with Bayer matrix (Athabasca University, 2018).

## Exposure times

Originally, exposure times of 40 seconds, 20 seconds, 10 seconds, and 5 seconds were requested from the DSO-17 telescope to determine the appropriate exposure time for this system. The AstroImageJ "source minus sky" photometry counts as a function of exposure time were investigated as a measure of image saturation. The photons represented by any given pixel of the image are counted by counting the electrons that are knocked loose from the corresponding pixel of the CCD camera attached to the telescope. Saturation occurs when the maximum number of electrons, usually 65,535, have been knocked loose from their corresponding pixel (Buchheim, 2007). These electrons are called "Analog-to-Digital Units" or ADU. AstroImageJ's "source minus sky" value is the total ADU count of all of the pixels within a circle on the image whose size is set by the user's selection of an aperture radius. An aperture radius of 14 pixels was chosen for the images of WDS 09144+5241 as it provided optimal coverage of the stars.

As shown in Figure 4, when a star is measured in AstroImageJ using the bullseye photometry tool, the total ADU count within the aperture radius appears in red next to the star on the image, and also in the measurement window as the "source minus sky" value. In cases where the circle covers a fraction of a pixel, the corresponding fraction of that pixel's ADU count is included in the sum. This technique for summing ADU counts from pixels within an aperture is called aperture photometry. If the pixels within an aperture are *not* saturated, the "source minus sky" value will be a linear function of the image exposure time.

The linearity of AstroImageJ's source-minus-sky count as a function of exposure time in the left-most regions of Figure 5 was taken as an indication that the stars' brightnesses were just beginning to saturate the CCD in the 20s exposure.

## Measurements and Astrometric Fitting

A second set of five 20s exposures was requested. These images, however, did not contain WDS 09144+5241. As shown in Figure 6, our star's coordinates of 09H 14M 22.79" +52° 41' 11.8" are beyond the extent of the image. Therefore, sets of images were re-requested from DSO-17, and also requested from DSO-

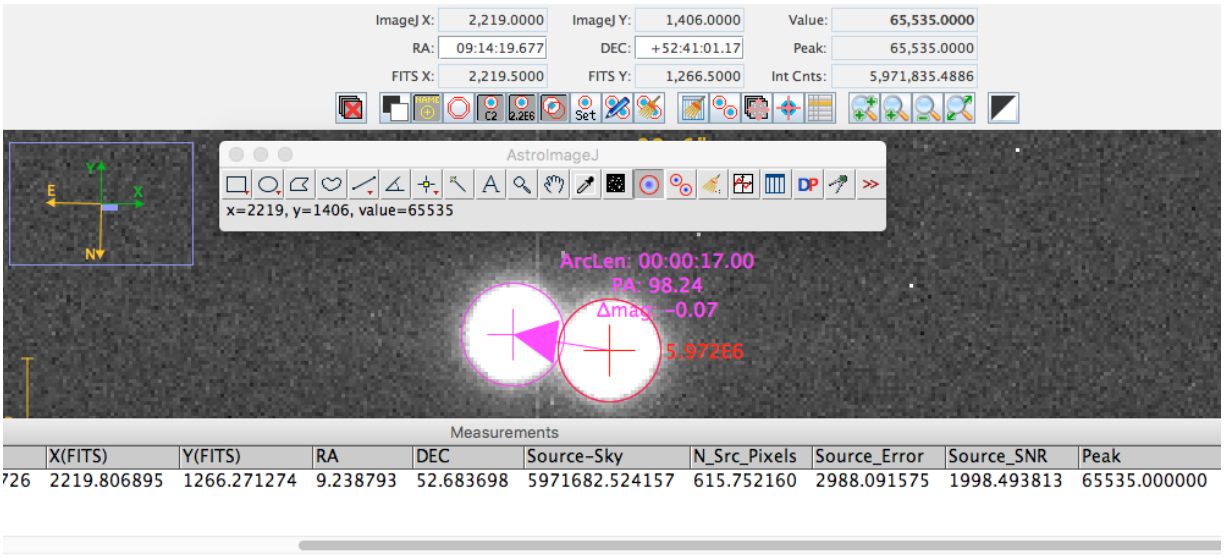


*Figure 4. AstroImageJ's aperture photometry count: shown in red next to the star being measured as well as in the measurement window below.*

14 and AURT as backups.

Although the next set of DSO-17 images once again did not contain the star, the returned DSO-14 and AURT images did. In the DSO-14 images, there were additional pixels of light near the top of the image, as shown in Figure 7. This "blooming" is an indication of image saturation.

Sometimes, when the maximum ADU count of a given pixel has been exceeded, excess photons will spill over onto adjacent pixels. In AstroImageJ, the ADU count for an individual pixel is represented by the number labeled "Value" in the upper right of the image window. This number changes as the mouse is moved over the pixels of the image, corresponding to the ADU count for that individual pixel. For the image shown in Figure 7, the count remained above 63,000 from the star centroid out to half its radius, and also exceeded 63,000 along the vertical spike. Because the ADU counts decreased as expected over the remainder of the star's image, we conclude that the saturation value for this camera is approximately 63,000 ADU counts per pixel.

The concern with saturation for double star astrometry is that for saturated images, it might become difficult for the software to locate the star centroid. The star centroid is the average position of the pixels within an aperture set by the user, weighted by the corresponding ADU count. If that count is artificially truncated at a maximum value, then the weighting will be incorrect. In Figure 7, the vertical blooming in the image drags the position of the centroid up higher than it would be if the electrons had not overflowed their buckets. For this image, since the blooming occurs in the same direction relative to both stars, the measurement is not as much affected as it might otherwise be. In fact, the measure-

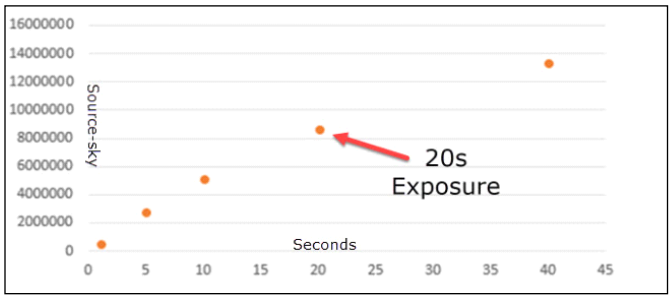


*Figure 5. AstroImageJ source-minus-sky photometry count as a function of exposure time for DSO-17 images of WDS 09144+5241.*

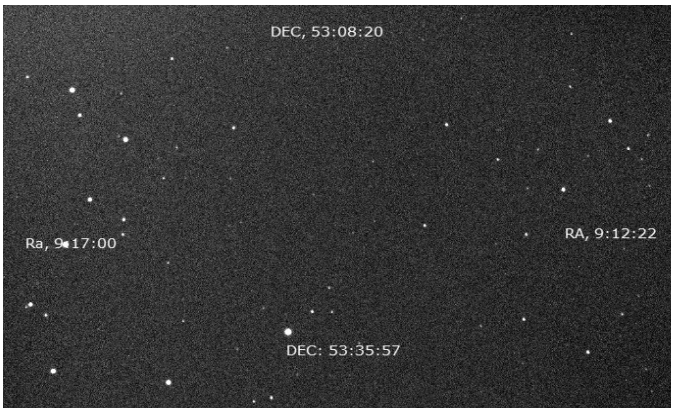


*Figure 6: A star field not containing WDS 09144+5241 with some labeled RA and Dec coordinates.*

# WDS 09144+5241: CCD Observations and Orbital Solutions

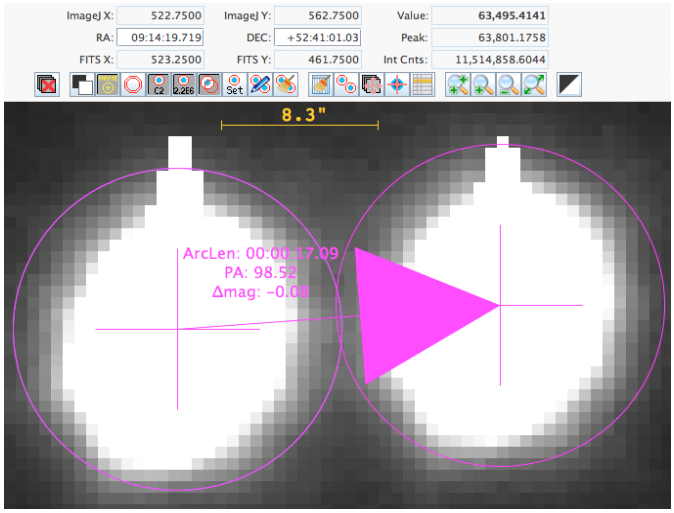


*Figure 7. A saturated, 20s exposure of WDS 09144+5241 from the DSO-14 telescope on Feb 9, 2018, aperture radius set at 14 pixels.*

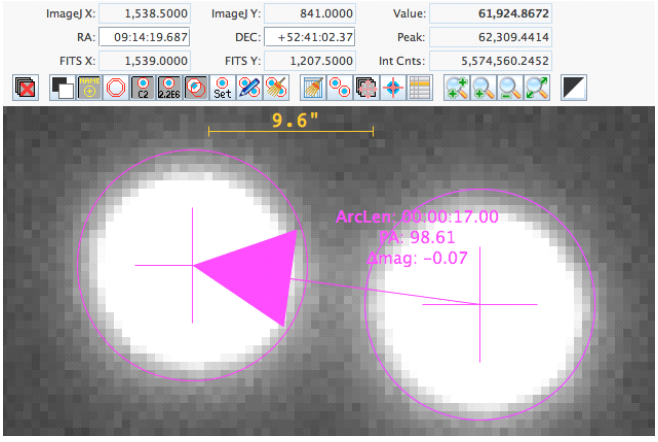


*Figure 8: Image of WDS 09144+5241 from the AURT telescope, showing pixel counts in the "Value" field close to but not exceeding saturation.*

ments made from this image were within a tenth of a degree in position angle (PA) and a tenth of an arcsecond in separation (Sep) from other images that were unsaturated. This is consistent with the work of Larsen et. al, who found that *unsaturated* images were more likely to be outliers in their astrometric measurements of double stars (Larsen, 2018).

Our first set of images from AURT had a WCS (World Coordinate System) registration failure, so the lack of a reliable plate solution rendered the images unusable. However, the second set had coordinates labeled, and the stars looked clear, as shown in Figure 8. The images were close to saturated (note the "Value" field of 61,924 when the mouse hovers near the centroid of the primary), but unlike the DSO-14 image, the decrease in electron count moving away from the star centroid was steady and monotonic. Some additional image requests with a 10s exposure time were made as a check of the measurement. Unfortunately, these images were taken and returned on the night of a full Moon, and were saturated despite the lowered exposure time.

Tables 2 and 3 show measurements made on all of the images we requested of this system. Despite the blooming evident on the DSO-14 images and the saturation of the April 28 images, the measurements were consistent with those made on the unsaturated images, as well as with our expectations based on the historical data taken from the Washington Double Star Catalogue. Because the measurements on saturated and unsaturated images were so similar, it appears that for these widely-separated stars, saturation did not affect the measure-

*Table 2: PA Measurements (in degrees) of WDS 09144+5241; unused, saturated images shaded.*

| | DSO-17 Jan 16, 2018 multiple exposure times, not saturated | DSO-14 Feb 9, 2018 20s exposures saturated (blooming) | AURT Feb 19, 2018 20s exposures, not saturated | DSO-17 Apr 28, 2018 10s exposures saturated (full moon) | DSO-14 Apr 28, 2018 10s exposures saturated (full moon) |
|---|---|---|---|---|---|
| | 98.08 | 98.52 | 98.56 | 98.28 | 98.39 |
| | 98.34 | 98.38 | 98.61 | 98.33 | 98.12 |
| | 98.52 | 98.40 | 98.57 | 98.33 | 98.15 |
| | 98.49 | 98.59 | 98.52 | 98.24 | 97.96 |
| | 98.41 | 98.47 | 98.52 | 98.24 | 98.23 |
| **Mean** | **98.37** | **98.47** | **98.56** | **98.28** | **98.17** |
| **SEM** | **0.079** | **0.039** | **0.017** | **0.020** | **0.070** |

**WDS 09144+5241: CCD Observations and Orbital Solutions**

*Table 3: Separation Measurements (in arcseconds) of WDS 09144+5241; unused, saturated images shaded.*

| | DSO-17 Jan 16, 2018 multiple exposure times, not saturated | DSO-14 Feb 9, 2018 20s exposures saturated (blooming) | AURT Feb 19, 2018 20s exposures, not saturated | DSO-17 Apr 28, 2018 10s exposures Saturated (full moon) | DSO-14 Apr 28, 2018 10s exposures Saturated (full moon) |
|---|---|---|---|---|---|
| | 17.01 | 17.09 | 16.99 | 17.02 | 17.04 |
| | 17.03 | 17.09 | 17 | 17 | 17.06 |
| | 16.96 | 17.08 | 17.03 | 17.02 | 17.07 |
| | 17.03 | 17.1 | 16.99 | 16.99 | 17.04 |
| | 17.01 | 17.09 | 17.01 | 17 | 17.06 |
| **Mean** | **17.01** | **17.09** | **17.00** | **17.01** | **17.05** |
| **SEM** | **0.013** | **0.003** | **0.007** | **0.006** | **0.006** |

ment adversely, also consistent with Larsen et. al. (Larsen, 2018). However, saturation may become a more important problem for stars that are closer together. The standard error of the mean for the separation of the stars was *lower* in the saturated images, making them more precise, even though they might be less accurate, than their unsaturated counterparts.

Although the saturated images yielded similar numerical values, we used the unsaturated for the analysis that follows.

## Ephemerides

The orbital solution of the system gives its ephemeris, or expected position, for several future dates. Selected ephemerides for WDS 09144+5241 are shown in Table 4.

Our DSO-17 measurement was made on the night of January 16, which is 16/365 of the year past the 2018.0 date for which the expected PA and Sep are listed. Therefore, we can find the expected values of PA and Sep on the night of January 16 by taking 16/365 of the difference between the expected values for 2019.0 and 2018.0, and adding this to the 2018.0 value. Similarly, the measurements with the AURT telescope on February 19 are expected to be 50/365 of the way between the 2018.0 and 2019.0 values. The ephemerides for the dates of our observations are compared to our measured PA and Sep values in Table 5.

When Bush's team carried out a similar calculation one year ago with their measurements of this system, they also found a lower PA and higher Sep than were predicted by the ephemeris. As with our data, the discrepancies were statistically significant because the ephemeris predicted PA and Sep values that were several multiples of the standard error away from the team's mean measurement (Bush, 2018).

*Table 4: Ephemerides for WDS 09144+5241 from the WDS Catalog.*

| Ephemerides | 2018.0 | 2019.0 |
|---|---|---|
| PA (°) | 98.8 | 99.2 |
| Sep (") | 16.807 | 16.785 |

## Orbital Solution

Figure 9 contains the complete historical data set from the Washington Double Star Catalog along with our DSO-17 and AURT telescope measurements and last year's measurement by Bush (Bush 2018). The zoomed-in plot on the right highlights the growing deviation of the most recent data points from the red line of Kyongae Chang's 1972 orbital solution (Chang, 1972). These plots were made by taking screenshots from the Desmos online graphing tool.

## Improvement Parameter

A common method for determining how well a proposed solution fits the data involves examining the residuals. The residuals are the distances between each data point and its corresponding expected position on the proposed solution. If the residuals are large, then the observed data points fall far away from their expected positions, implying that the proposed solution is not a good explanation for the measurements.

*Table 5: Distance (in standard errors) between our measurements and the ephemerides for WDS 09144+5241 on Jan 16 and Feb 19.*

| Measurement | Number of SEMs between our mean measurement and ephemerides for Jan 16 | Number of SEMs between our mean measurement and ephemerides for Feb 19 |
|---|---|---|
| PA (degrees) | 5.7 | 17.3 |
| Sep (arcseconds) | -15.7 | -29.0 |

**WDS 09144+5241: CCD Observations and Orbital Solutions**

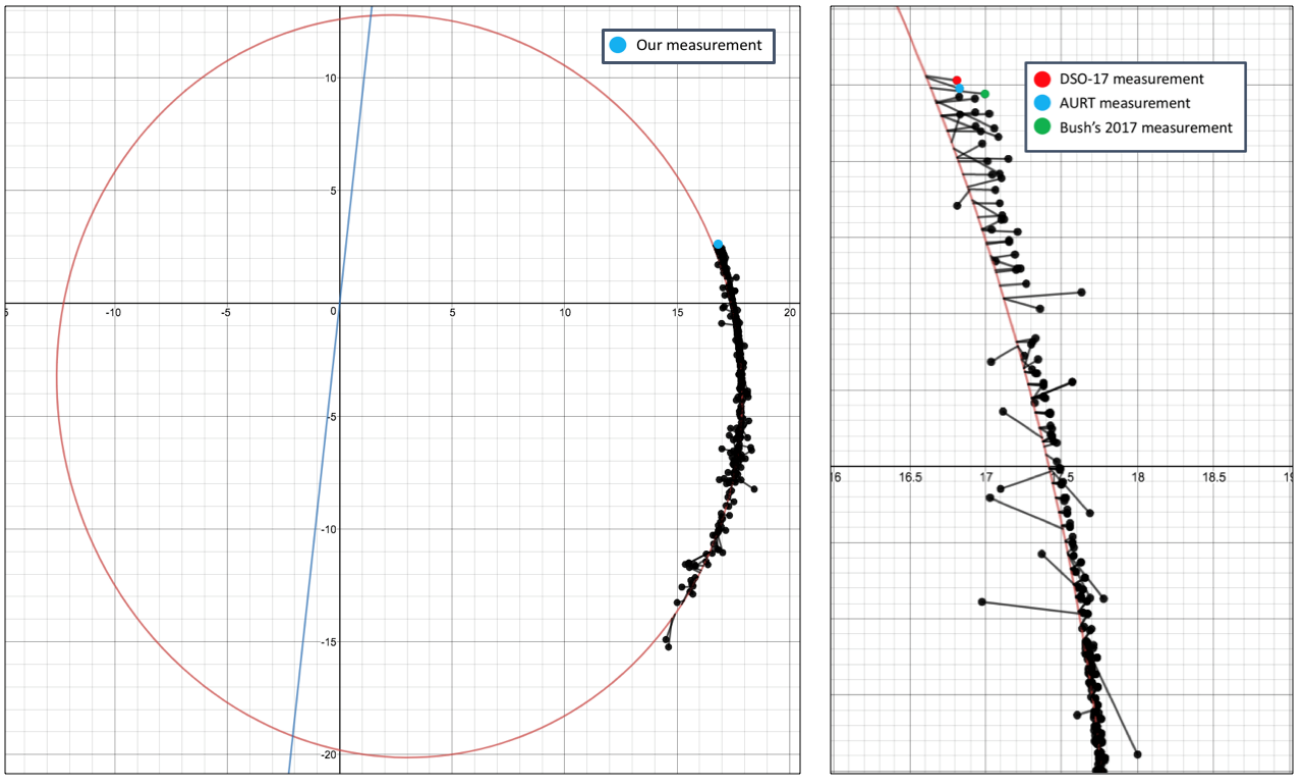


*Figure 9. Our measurements of WDS 09144+5241 from the DSO-17 and AURT telescopes, along with Bush's 2017 measurement, in the context of the historical data for this system.*

The coefficient of determination, $R^2$, is defined as $1 - SS_{res}/SS_{tot}$, where $SS_{res}$ is the sum of squares of the residuals, and $SS_{tot}$ is the sum of squares of the distances of each point from the average position of all data points. If $SS_{res}$ is smaller than $SS_{tot}$, that means that the measurements fall closer to the proposed solution than they do to the average position of the data points, and $R^2$ will be close to 1. Therefore, an $R^2$ close to 1 implies that the data points are less likely to be explained by random scatter around their mean position than they are to be explained by the proposed solution.

As we can see, the coefficient of determination takes into account the squared magnitude of the residuals, but taking the square causes information to be lost. For example, consider the two fits shown in Figure 10. Although they have similar $R^2$ values, the fit on the left shows a clear pattern to the residuals. By contrast, the fit on the right has residuals that are scattered with respect to the fit.

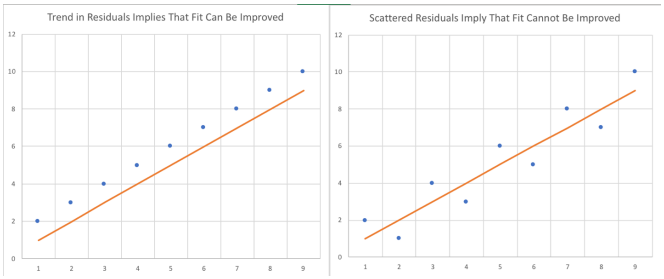


*Figure 10: Two linear fits.*

It is clear from visual inspection that while a linear fit is appropriate in both cases, the fit on the left could be improved by adjusting one of the two parameters of the line: namely, the y-intercept. The pattern in the residuals, which are all to the same side of the fit, allows us to detect the needed parameter adjustment. For an orbital solution such as that of WDS 09144+5241, however, it is sometimes less obvious which of the seven orbital parameters could be adjusted to improve the fit, or even whether improvement is possible.

To determine whether the residuals of a seven-dimensional orbital solution exhibit a pattern, the residuals *themselves* can be fit to a third-order polynomial function. We define the "improvement parameter" to be the $R^2$ value of the best fit of the residuals to this function. An improvement parameter close to 0 indicates that the residuals are scattered, and the orbital pa-

**WDS 09144+5241: CCD Observations and Orbital Solutions**

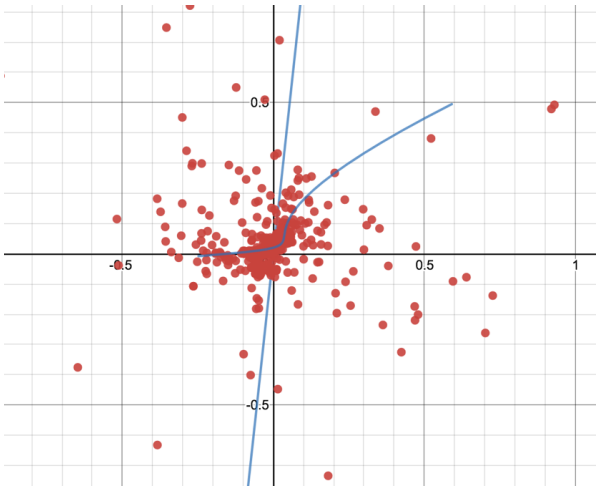


**Chang's Orbital Fit Parameters**

a = 16.725
$e_0$ = 0.28
i = 21
Ω = 353.8
ω = 44
M = 264
p = 975

$R^2$ = 0.9956
Improvement parameter = 0.18

Link: tiny.cc/changsoln

*Figure 11: Residuals mapped around the primary star for Chang's orbital solution for WDS 09144+5241.*

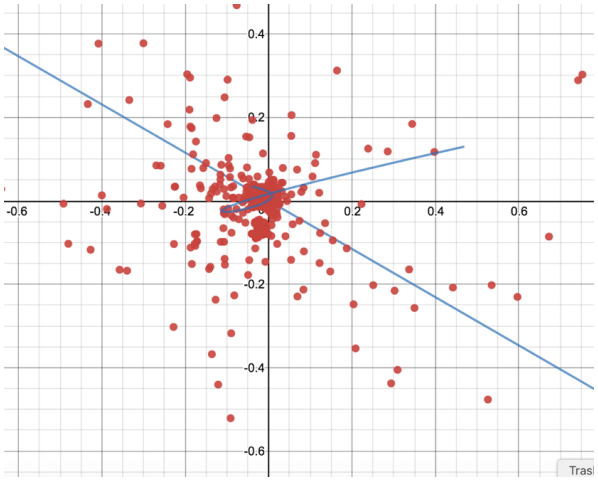


**Our Best Orbital Fit Parameters**

a = 19.682
$e_0$ = 0.19822
I = 11.18
Ω = 239.99
ω = 98
M = 314.66
p = 1423.93

$R^2$ = 0.9961
Improvement parameter = 0.05

Link: tiny.cc/bestip

*Figure 12: Residuals for our best, unweighted orbital solution for WDS 09144+5241.*

rameters are as good as they are going to get. However, if the residuals have an $R^2$ above about 0.1 for the best fit polynomial, that indicates that they exhibit some sort of pattern, and the overall fit can be improved in some way.

On Figure 11, the unweighted residuals of the 550 data points for WDS 09144+5421 are visualized as projections mapped around the primary star (only three of the most egregious outliers were removed). The parameters of Chang's orbital solution with these 550 data points have a very high $R^2$ of 0.9956. The $R^2$ would likely be even higher if the observations had been weighted according to the Washington Double Star Catalog weighting scheme (US Naval Observatory, 2018). The curved blue line in the center of the plot shows the third-order polynomial trendline for the improvement parameter. Its $R^2$ value is 0.18, which indicates that the residuals exhibit a slight trend.

The residuals and parameters of a better-fitting orbital solution are shown in Figure 12. That the residuals are close to the primary star and randomly distributed around it in all directions indicates that this improvement parameter will be small, and indeed it has value 0.05. This fit has an $R^2$ of 0.9961. Although the $R^2$ is similar to Chang's, the corresponding zoomed-in fit shown in Figure 13 does *not* show the increasing deviation of the measurements with time that was apparent in Figure 9.

This example demonstrates that the $R^2$ value alone is an incomplete means of assessing the accuracy of a fit, because it disregards information that can be gleaned from examining patterns in the residuals.

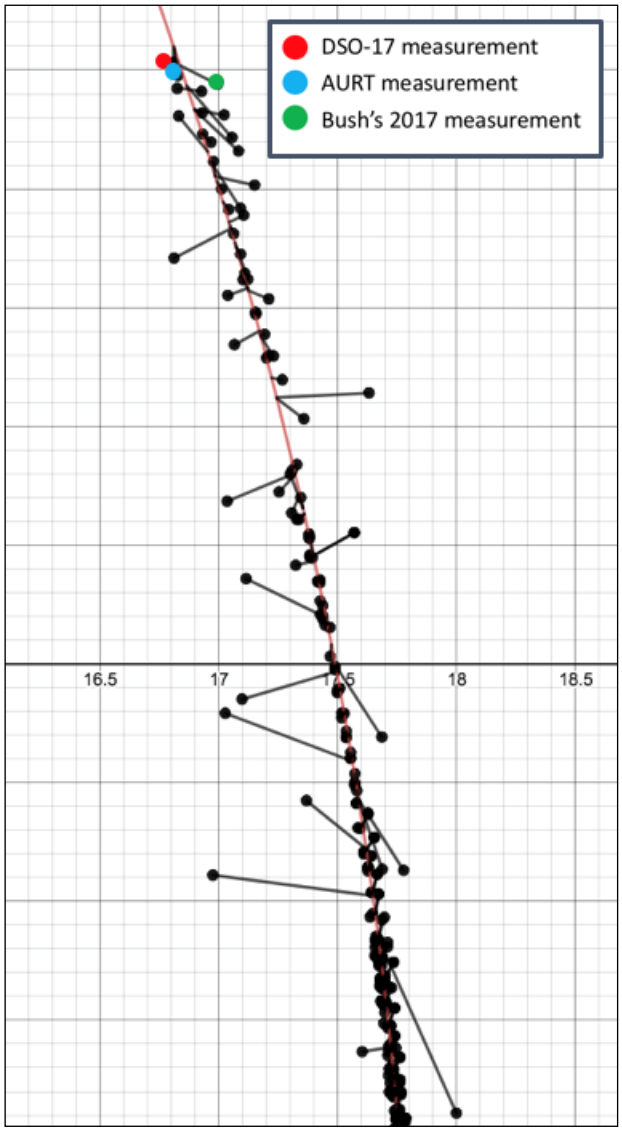


*Figure 13: Zoomed-in plot of our best, unweighted orbital solution for WDS 09144+5241.*

From the improvement parameter, we can tell that Chang's solution, with its high $R^2$ of 0.9956, can still benefit from adjustment. For other systems, such as those with an even shorter arc and significant noise, the best $R^2$ might be quite low, with no improvement possible (i.e. no pattern to the residuals). The improvement parameter, defined as the fit of the residuals themselves to a third-order polynomial function, provides a useful means of testing for this.

## Orbital solutions

The differences between Chang's solution and our best orbital solution highlights the range of uncertainty in the parameters, even for fits with high $R^2$ values. Using 50 data points spanning the 200 years that the system has been observed, we found a number of orbital solutions in the Desmos orbital solution tool (Hensley, 2018). To get the solutions, we moved the sliders for the parameter values such that the $R^2$ value in Desmos came as close to 1 as possible. Using 50 data points rather than all 550 of the observations for this system allows Desmos to run significantly faster, and makes manipulation of the sliders easier. The 50 points were selected manually by skimming through the data in Excel, taking one non-outlier point per rough time period.

For a somewhat short arc such as WDS 09144+5241, which covers only a fraction of the entire orbit, it is often possible to find not just one solution, but an entire family of solutions that give a close fit along the observed arc but differ significantly over the remainder of the orbit. Since the goodness of fit seems to be a smooth, locally linear function of each parameter, it seems reasonable to think that the entire family of solutions might lie along a smooth curve in seven-dimensional space. Using a second-order polynomial fit through three similarly high-$R^2$ solutions, one of us (Hensley) found that this seems to be the case, and parameterized a subset of the family of solutions in terms of a parameter v. Various solutions in this family are shown in Table 6. Each one of these solutions exhibits a very different value of each parameter. The period, for example, could be anywhere within a range of almost 700 years. Yet these are all perfectly good solutions, with an $R^2$ of 0.995 or higher. This method could prove useful for incorporating future observations into a refined orbital solution. Since all of the solutions in the table begin to vary significantly for points in the future, an observation not even that far into the future (10 or 20 years might suffice) could be used to narrow down the value of the parameter v.

## Conclusion

WDS 09144+5241 STF 1321 AB is considered a short-arc binary and a grade 4 physical double. Using multiple telescopes through Skynet, we measured its position angle and separation. Using the 550 past observations of WDS 09144+5241 together with our own observations, we identified a trend in the residuals that enabled us to improve the $R^2$ value of the unweighted fit.

## Acknowledgements

This research has made use of the Washington Double Star Catalog maintained at the U.S. Naval Observatory, the SkyNet Robotic Telescope Network, the Stelledoppie catalogue maintained by Gianluca Sordi-

## WDS 09144+5241: CCD Observations and Orbital Solutions

*Table 6: Possible Desmos fit parameters for a 50-point subset of data for WDS 09144+5241.*

| | v = 0 solution | v = 0.2 solution | v = 0.4 solution | v = 0.6 solution | v = .08 solution | v = 1 solution |
|---|---|---|---|---|---|---|
| **a** | 23.8 | 22.4 | 21.2 | 20.3 | 19.5 | 18.9 |
| **e** | 0.35 | 0.24 | 0.23 | 0.22 | 0.21 | 0.20 |
| **i** | 20 | 14.8 | 11.2 | 9.2 | 8.8 | 10 |
| **Ω** | 212 | 221 | 230 | 238 | 245 | 252 |
| **⍰** | 90 | 91.6 | 93.2 | 94.8 | 96.4 | 98 |
| **M** | 343.5 | 335.9 | 328 | 320.4 | 312.5 | 304.5 |
| **p** | 2000 | 1823 | 1666 | 1527 | 1408 | 1308 |
| **$R^2$** | 0.995 | 0.995 | 0.996 | 0.996 | 0.997 | 0.997 |
| **Link** | tiny.cc/soln0 | tiny.cc/soln1 | tiny.cc/soln2 | tiny.cc/soln3 | tiny.cc/soln4 | tiny.cc/soln5 |
| Fig | 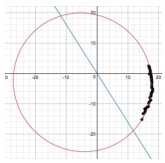 | 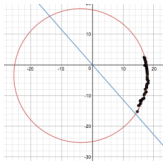 | 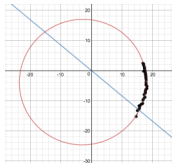 | 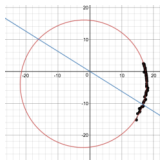 | 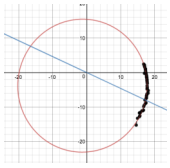 | 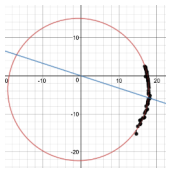 |

glioni, and AstroImageJ software written by Karen Collins and John Kielkopf at the University of Louisville, updated for double star astrometry by Karen Collins.

This work has also made use of data from the European Space Agency (ESA) mission Gaia (https://www.cosmos.esa.int/gaia), processed by the Gaia Data Processing and Analysis Consortium (DPAC, https://www.cosmos.esa.int/web/gaia/dpac/consortium). Funding for the DPAC has been provided by national institutions, in particular the institutions participating in the Gaia Multilateral Agreement.

Special thanks to Richard Harshaw for inspiring our class as we commenced this project in January and answering our numerous scientific questions as we sallied forth on this scientific adventure with many twists and turns.

## References

Athabasca University Robotic Telescope (AURT), 2018. Retrieved from http://augo.athabascau.ca/information/aurt/ May 2018.

Bush, Mitchell and Eric Del Medico, Hunter Boulais, Christina Lang, Jesus Escalante Segura, Sara D'ambrosia, David Rowe, Rachel Freed, Russell Genet, 2018. "Astrometry Observations of STF 1321AB". Journal of Double Star Observations. Retrieved in May 2018 from http://www.jdso.org/volume14/number1/Bush_38_42.pdf

Chang, Kyongae, 1972. "Parallax, proper motion, and orbital motion of the visual binary SIGMA 1321". Astronomical Journal, Vol. 77, p. 759 - 761. Retrieved in April 2018 from http://cdsads.u-strasbg.fr/cgi-bin/nph-iarticle_query?letter=.&classic=YES&bibcode=1972AJ.....77..759C&page=&type=SCREEN_VIEW&data_type=PDF_HIGH&send=GET&filetype=.pdf

Encyclopaedia Britannica, 1998. "Friedrich Georg Wilhelm von Struve: Russian Astronomer". Retrieved in Feb, 2018 from https://www.britannica.com/biography/Friedrich-Georg-Wilhelm-von-Struve.

Buchheim, Robert, 2007. "Astronomical Discoveries You Can Make, Too! Replicating the Work of the Great Observers." Praxis Publishing, Chichester, UK. ISBN 978-3-319-15659-0. 2007.

Harshaw, Richard, 2014. "Another Statistical tool for evaluating Binary Stars". Retrieved in April, 2018 from http://www.jdso.org/volume10/number1/Harshaw_32_51.pdf

Harshaw, Richard, 2016. "CCD Measurements of 141 Proper Motion Stars: The Autumn 2015 Observing Program at the Brilliant Sky Observatory, Part 3". Retrieved in April, 2018 from http://www.jdso.org/volume12/number4/Harshaw_394_399.pdf

Harshaw, Richard, 2014. "The Fascinating World of The Short Arc Binaries". Retreived in Feb, 2018 from http://www2.lowell.edu/workshops/speckle2014/presentations/05-02%20harshaw%20-%20Lowell%20Conference%20SABs.pdf

Hartkopf, William, Brian D. Mason, and Charles E. Worley. "The 2001 US Naval Observatory Double Star CD-ROM. The Fifth Catalog of Orbits of Visual Binary Stars.", The Astronomical Journal, 122: 3472 – 3479, 2001. Retrieved from http://iopscience.iop.org/article/10.1086/323921/fulltext/

Hensley, Hagan, 2018. "The Orbital Solution Initial Value Problem". Journal of Double Star Observations: Vol 14 No 2, 2018, pp. 353-356. Retrieved from http://www.jdso.org/volume14/number2/Hensley_353_356.pdf

Larsen, Skylar, Schuyler Smith, Jerry Hilburn, and Pat Boyce, 2018. "Investigation into the Accuracy of Small Telescope CCD Astrometry of Visual Double Stars", The Society of Astronomical Sciences: Proceedings for the 37th Annual Symposium on Telescope Science and Association of Lunar and Planetary Observers Annual Meeting, June 14 – 16, 2018.

Smith, Adam Blythe, 2009. "The Development and Implementation of a Remote Robotic Telescope System at Appalachian State University's Dark Sky Observatory: A Thesis". Retrieved in May 2018 from https://dso.appstate.edu/sites/dso.appstate.edu/files/thesis.pdf.

Skynet. "AURT" telescope. Retrieved in Feb, 2018 from https://skynet.unc.edu/telescopes/view?id=2

Skynet. "DSO-14" telescope. Retrieved in Feb, 2018 from https://skynet.unc.edu/telescopes/view?id=5

Skynet. "DSO-17" telescope. Retrieved in Feb, 2018 from https://skynet.unc.edu/telescopes/view?id=6

US Naval Observatory website, "The Sixth Catalog of Orbits of Visual Binary Stars", retrieved May 2018 from http://ad.usno.navy.mil/wds/orb6/orb6text.html

Wikipedia contributors, 2017. "Dark Sky Observatory". Retrieved in Feb, 2018 from https://en.wikipedia.org/wiki/Dark_Sky_Observatory

Wikipedia contributors, 2017. "Friedrich Georg Wilhelm von Struve". Retrieved in Feb, 2018 https://en.wikipedia.org/wiki/Friedrich_Georg_Wilhelm_von_Struve

World Heritage Centre, 2018. "Struve Geodetic Arc". Retrieved in March 2018 from https://whc.unesco.org/en/list/1187